ACS Macro Letters

Letter

pubs.acs.org/macroletters

# Diblock Copolymer Grafted Particles as Compatibilizers for Immiscible Binary Homopolymer Blends

Carla E. Estridge[†,‡] and Arthi Jayaraman*[,‡,§]

[†]Department of Chemistry and Biochemistry, University of Colorado, Boulder, Colorado 80309, United States

[‡]Department of Chemical and Biomolecular Engineering, University of Delaware, Newark, Delaware 19716, United States

[§]Department of Materials Science and Engineering, University of Delaware, Newark, Delaware 19716, United States

Supporting Information

**ABSTRACT:** Using coarse-grained molecular simulations we study AB diblock copolymer grafted particles (DBCGPs) as compatibilizers in an immiscible blend of A and B homopolymers. The fraction of the A block in the graft, $f_A$, tunes the location of the DBCGPs within the blend. When $f_A$ = 0.25, the DBCGPs preferentially localize in the B domain of the blend, and when $f_A$ = 0.5 and 0.75, the DBCGPs localize at/near the interface of the A and B domains, adopting conformations that segregate the A and B segments of the grafts into chemically identical domains of the blend. The desorption energy to leave the interface and the drop in interfacial tension are larger for the DBCGP than ungrafted diblock copolymers, commonly used as compatibilizers. Additionally, the comparable reduction in interfacial tension of DBCGPs as Janus-homopolymer grafted particles, along with the easier synthesis routes of DBCGP, makes DBCGP an attractive alternative class of compatibilizers for polymer blends.

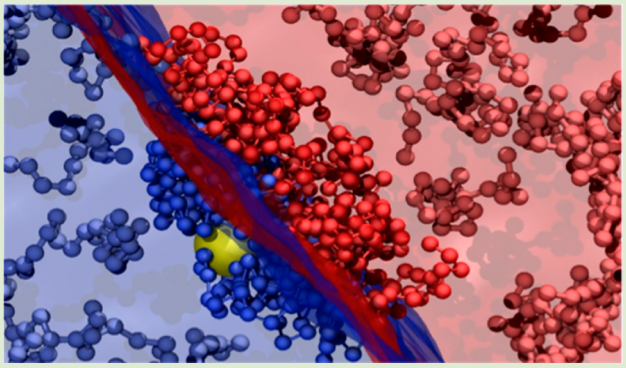

Many industrial applications require blending of immiscible polymers to create materials with superior properties. In blends of immiscible homopolymers macrophase separation of the component polymers leads to formation of domains. The interfaces between domains can reduce processability of the blend[1] and create mechanical instability in the processed material.[2] To stabilize such interfaces, compatibilizers are added to reduce interfacial tension between the two immiscible polymers and to increase interfacial adhesion.[3,4] One class of commonly used compatibilizers for blends of A and B homopolymers are AB diblock copolymers (BCPs).[3] One limitation of BCPs is that beyond a critical concentration, in addition to localizing at the interfaces, BCPs aggregate and form micelles within the homopolymer domains.[4] Micellization introduces new heterogeneous interfaces within the blend that can negatively impact material performance. Additionally, BCPs can be lost during blend processing, such as high shear extrusion.[5] Another class of compatibilizers is nanoparticles. Nanoparticles with nonselective interactions toward the blend homopolymers localize at the polymer−polymer interface when the entropic loss of the nanoparticles upon localization at the interface is compensated by shielding of enthalpically unfavorable contacts between the two homopolymer components of the blend.[6] Nanoparticles grafted with homopolymer(s) prepared by both "grafting through"[7] and "grafting from"[8] methods have also been shown to localize at oil−water interfaces reducing the interfacial tension and stabilizing emulsions. Janus-like grafting on the nanoparticle surface to selectively interact with each of the blend polymers leads to enthalpically driven stabilization of the particles at the blend polymer−polymer interfaces[9] and improved interfacial stability over BCPs.[10] However, these interfacially superior Janus particles are challenging to synthesize making the extension for use in large-scale industrial processes difficult.[11−14]

In this work, using molecular simulations we demonstrate that AB *diblock copolymer grafted nanoparticles* (DBCGPs) are an excellent alternative to BCPs and Janus nanoparticles for compatibilization of immiscible A and B polymer blends. We show that DBCGPs preferentially locate at the interfaces between macrophase-separated domains and reduce interfacial tension without the issues of BCPs' micellization. Additionally, others show that the synthesis of DBCGPs is relatively less complex compared to the Janus nanoparticles.[15,16] We show that as the fraction of the grafted A block in the graft copolymer ($f_A$) increases the probability of DBCGP localization at the interface of the polymer domains increases. Comparisons of interfacially located DBCGPs to that of BCPs and Janus homopolymer grafted particles (JGPs) show that (a) DBCGPs have higher desorption energy from the interface as well as a significantly higher reduction of interfacial tension than BCPs and (b) JGPs, as expected, show the largest desorption energy

**Received:** December 11, 2014
**Accepted:** January 8, 2015
**Published:** January 13, 2015

  

DOI: 10.1021/mz500793e
*ACS Macro Lett.* 2015, 4, 155−159

from the interface and largest reduction in interfacial tension compared to both BCPs and DBCGPs. However, considering the synthetic limitations of JGPs, the large desorption energy from the interface and reduction in interfacial tension exhibited by DBCGP make DBCGPs a more viable option for compatibilization of polymer blends.

In Figure 1a we show the effect of graft composition ($f_A$) on the average location of the DBCGP at low DBCGP volume fraction ($\phi$) after macrophase separation of the immiscible homopolymer blend. The DBCGPs have a particle diameter $D = 4\sigma$ (where $\sigma \sim 1$ nm) with A−B diblock copolymers of $\chi \propto \varepsilon_{AB} - 1/2(\varepsilon_{AA} + \varepsilon_{BB}) \approx 1$ and length $N_{graft} = 24$ beads (Kuhn segments) grafted at 0.51 chains/$\sigma^2$ and placed in a symmetric blend of A and B homopolymers with $N_{blend\_A\_homopolymer} = N_{blend\_B\_homopolymer} = 24$ beads. The particle size $D$ is commensurate with the radius of gyration of the grafts, $\langle R_g^2 \rangle^{1/2}$. At $f_A = 0.25$ and $\phi = 0.004$ the DBCGP preferentially migrates to the B domain with the graft A segments aggregating near the particle surface and the graft B segments interacting with the blend's B domain (Figure 1b, left). This configuration maximizes the enthalpically favorable graft-blend B−B contacts while shielding the graft A beads from the blend B beads and allowing graft A beads to form enthalpically favorable contacts within the grafted layer. At $\phi = 0.1$, the DBCGPs preferentially fill the B domain, and few DBCGPs localize at the interface (Supporting Information, Figures S.1 and S.2) The DBCGPs at the interface take on graft configurations facilitating the graft A (B) beads to interact with the blend A (B) beads (Figure 1b, right). Despite these enthalpically favorable contacts, this interfacial state is not preferred at lower concentration because it decreases the grafts' conformational entropy as they stretch around the particle to make these energetically favorable contacts. The fraction of the DBCGPs that go to the interface will depend on the size of the macrophase-separated domains.

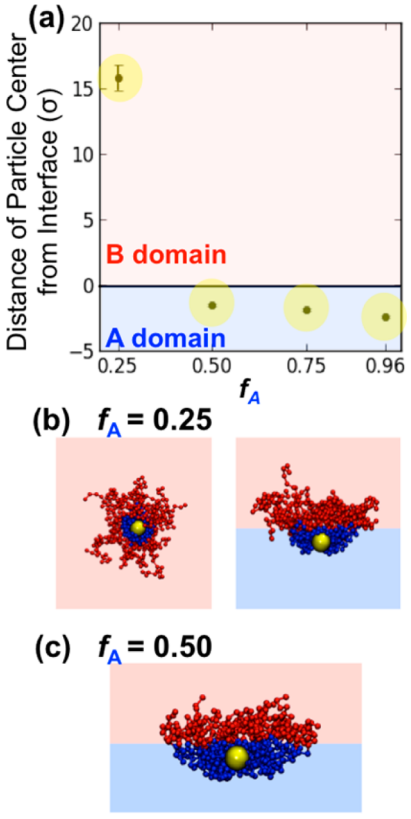


**Figure 1.** DBCGP conformations and location in the blend. (a) Average particle distance from the interface (in units of $\sigma \sim 1$ nm) versus $f_A$, where $f_A = N_A/(N_{A+B})$ with $N_A$ being the number of A monomers in the diblock copolymer and $N_{A+B} = N_{graft} = 24$, at $\phi = 0.004$, where $\phi$ is the total volume of the DBCGP divided by the simulation box volume. Yellow circle is the size of the nanoparticle core. Error bars are standard error. Representative simulation snapshots of (b) $f_A = 0.25$ DBCGP in B domain and at interface and (c) $f_A = 0.50$ DBCGP at the interface.

At $f_A = 0.50$ and $\phi = 0.004$ the DBCGP preferentially migrates to the interface, with the center of the particle slightly offset from the interface within the A domain and the A and B portions of the grafted layer segregating into the A and B domains of the blend (Figure 1c) to maximize energetically favorable interactions. This configuration of grafted particles near the interface is in agreement with recent *theoretical studies* of similar systems at lower grafting density[17] (for differences between our molecular simulation and other theoretical approaches see Supporting Information). As $\phi$ increases, all the $f_A = 0.50$ DBCGPs localize near the interface (Supporting Information, Figure S.3). At $f_A = 0.75$, at *all* $\phi$ considered, the DBCGPs preferentially localize near the interface with similar configurations as $f_A = 0.50$ (Figure 1a and Supporting Information Figure S.4). In contrast to $f_A = 0.50$, due to a larger number of grafted A beads the $f_A = 0.75$ DBCGPs cores are more offset from the interface and in the A domain. At $f_A = 0.96$, where each graft has only 1 (end) B bead and 23 A beads, surprisingly, DBCGPs still localize near the interface with the particle center located farther from the interface than at $f_A = 0.50$ or 0.75.

Having established the preferred location of these DBCGPs, next we seek to understand the *interfacial activity* of $f_A = 0.50$ and 0.75 DBCGPs by comparing to two other interfacial compatibilizers—ungrafted symmetric diblock copolymers (BCPs) and Janus homopolymer grafted particles (JGPs). The length of the symmetric BCPs is equal to that of the grafted diblock copolymers on the $f_A = 0.50$ DBCGPs, and the number of BCPs added is equal to the number of grafted copolymers in the corresponding DBCGP simulation at the specific $\phi$. JGPs have the same grafting density, total number of A and B beads, and approximately the same (homopolymer) graft lengths as those in the $f_A = 0.50$ DBCGPs. For each of the four cases, $f_A = 0.50$ DBCGPs, $f_A = 0.75$ DBCGPs, JGPs, and BCPs, we vary $\phi = 7.3 \times 10^{-4}$ to $1.4 \times 10^{-2}$ while maintaining the interfacial area constant at $60 \times 60\ \sigma^2$ (see simulation protocol in Supporting Information).

Snapshots of the various compatibilizers located at the interface with increasing $\phi$ are in Figure 2 and Supporting Information Figures S.5−8. Figure 3 presents the effect of increasing $\phi$ on compatibilizer distance from the interface and conformations of DBCGPs, JGPs, and BCPs. For all $\phi$'s considered here, the DBCGP centers are located farther from the interface than JGPs and BCPs. This is because the A grafted block of the DBCGP forces the particle to localize in the A domain of the blend to maximize A−A contacts between grafts and blend (Figure 3b, left). JGPs, however, localize directly at the interface allowing all the A (B) homopolymers grafted on one (other) hemisphere of the particle to interact with the A (B) domain of the blend (Figure 3b, right). These graft conformations are quantified via the principle moments of the radius of gyration tensor averaged over the individual grafted particles located at the interface. For both $f_A = 0.50$ and $f_A =$


DOI: 10.1021/mz500793e
ACS Macro Lett. 2015, 4, 155−159

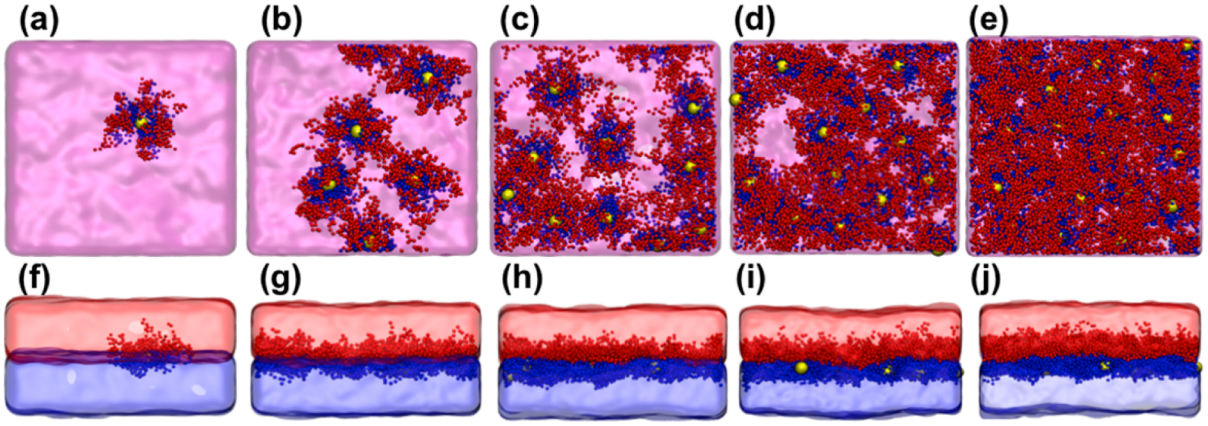


**Figure 2.** Interfacial configurations. Representative snapshots of interfacial coverage of $f_A = 0.5$ DBCGPs at (a,f) $\phi = 7.3 \times 10^{-4}$, (b,g) $\phi = 3.6 \times 10^{-3}$, (c,h) $\phi = 7.3 \times 10^{-3}$, (d,i) $\phi = 1.0 \times 10^{-2}$, and (e,j) $\phi = 1.4 \times 10^{-2}$. Top view through the B portion of the blend and side view of the interface are shown.

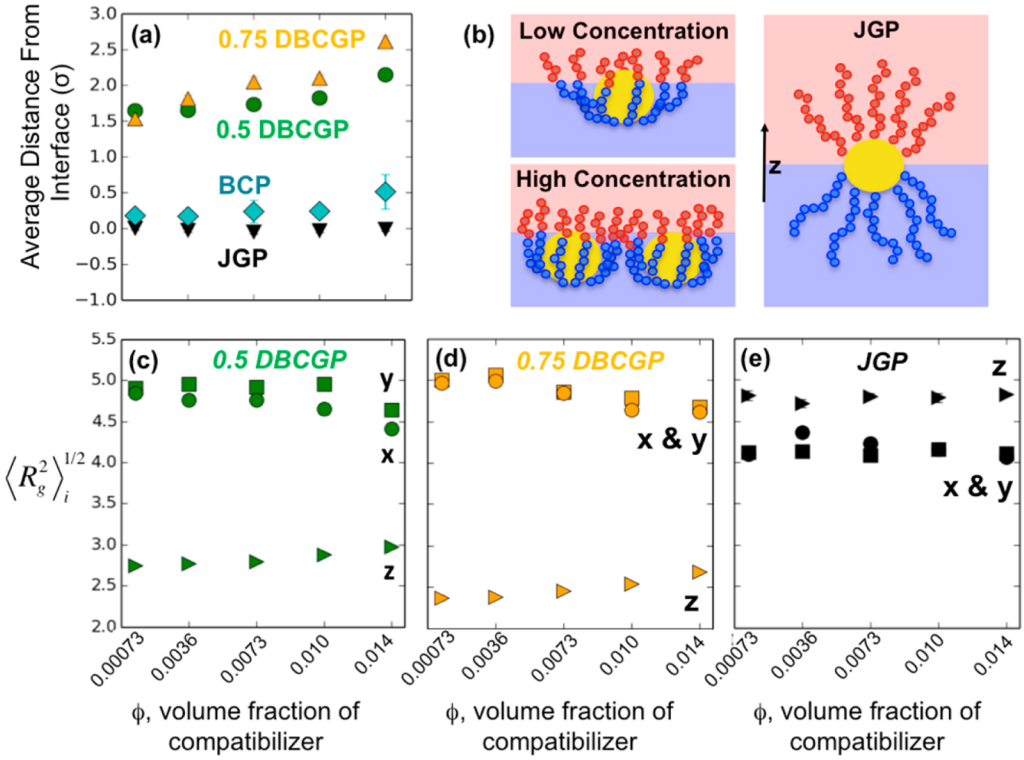


**Figure 3.** Location and conformations of the compatibilizers. (a) Average distance of the compatibilizer from the interface versus $\phi$ (same x-axis as c). (b) Schematics of DBCGP configurations and JGP configuration at the interface. (c–e) Average principle moments of the radius of gyration tensor versus $\phi$ for (c) $f_A = 0.50$ DBCGP, (d) $f_A = 0.75$ DBCGP, and (e) JGP. Standard error is plotted.

0.75 DBCGPs (Figure 3c,d) the two components of $\langle R_g^2 \rangle^{0.5}$ tangential to the interface ($x$ and $y$) are larger than the normal component ($z$), suggesting an oblate spheroid configuration of the DBCGP. As $\phi$ increases, crowding of the particles at the interface causes the grafted layer to extend in the $z$ direction while shrinking in the $x$ and $y$ directions (Figure 3b, left). The increase in $\langle R_g^2 \rangle_z^{0.5}$ with increasing $\phi$ is larger for $f_A = 0.75$ than $f_A = 0.50$ because the larger grafted A block in the former forces the core further into the A domain making the grafts adopt more elongated configurations to facilitate favorable like-monomer enthalpic contacts. For $f_A = 0.75$ DBCGPs at high $\phi$ some *grafts* localize fully in the A domain (Supporting Information Figure S.9), likely to relieve conformational entropic losses at the cost of a small enthalpic penalty.

Unlike DBCGPs, JGPs adopt a prolate spheroid configuration of the grafts (Figure 3e) that is relatively insensitive to $\phi$, at these low $\phi$. The higher $z$ component arises from the grafts of JGP penetrating the two domains of the blend more deeply than the DBCGPs. Comparison of the $x$ and $y$ components shows that JGPs occupy smaller interfacial area per particle than the DBCGPs do, justifying the insensitivity to lateral crowding due to increasing $\phi$. Symmetric BCPs also localize at the interface, but unlike JGPs, with increasing $\phi$ the average distance of the BCP centers from the interface increases because some of the BCPs leave the interface and micellize, as expected experimentally[5] and confirmed computationally by us (Supporting Information Figure S.10).



DOI: 10.1021/mz500793e
*ACS Macro Lett.* 2015, 4, 155−159

We present the energy associated with removal of a single compatibilizer from the interface in Figure 4 (see details of

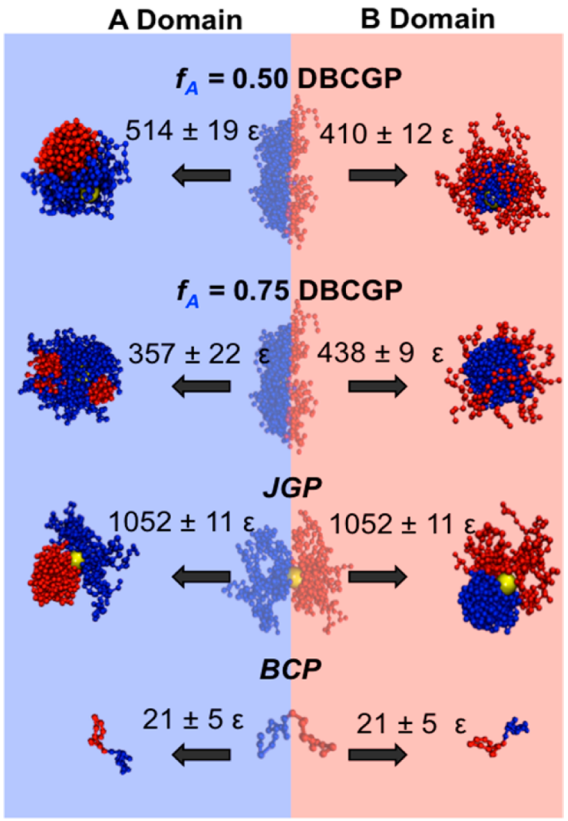


**Figure 4.** Energetic penalty for leaving the interface. Representative snapshots of compatibilizer configurations at the interface and within each domain and the desorption energies associated with each case.

calculation in Supporting Information). Unlike the symmetric JGPs and BCPs, the $f_A$ = 0.50 and 0.75 DBCGPs have different desorption energies going from interface to A and B domains due to asymmetry caused by A being the inner block and B being the outer block in the grafts. Because of this asymmetry, when found in the A domain the DBCGPs take on patchy configurations, while in the B domain they take on (A)core−(B)corona configurations[18] leading to the desorption energy of $f_A$ = 0.50 DBCGP into the B domain being lower than that into the A domain. Conversely, the desorption energy of $f_A$ = 0.75 DBCGPs into the A domain is significantly lower than that into the B domain, due to higher number of A beads in the grafted layer. These differences in desorption energy to either domain are not seen in the JGPs and BCPs due to symmetric configurations and equal amount of A and B beads. JGPs have the largest desorption energy due to the deeper penetration of the grafted beads into the A and B homopolymer domain of the blend. The DBCGP desorption energy is larger than the BCP, and therefore DBCGPs are more stable at the interface than BCPs.

Comparison of average interfacial tension of the compatibilized blend ($\gamma$) normalized by blend without compatibilizers ($\gamma_0$) versus $\phi$ for the interfacial area of 60 × 60 $\sigma^2$ shows that the JGPs have the lowest $\gamma/\gamma_0$ at all $\phi$ considered (Figure 5). Interestingly, both compositions of DBCGPs also reduce the interfacial tension comparable to JGP, with the $f_A$ = 0.50 DBCGP showing significantly larger reduction than $f_A$ = 0.75.

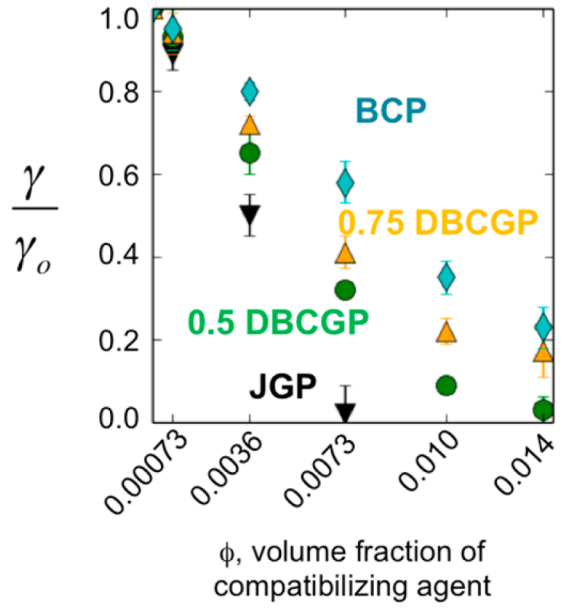


**Figure 5.** Reduction in interfacial tension. Ratio of compatibilized blend interfacial tension ($\gamma$) to compatibilizer-free blend interfacial tension ($\gamma_0$) versus $\phi$. Error bars are standard error.

This is due to $f_A$ = 0.50 DBCGPs' location near the interface and the large cross-sectional area ($x$ and $y$ component of $\langle R_g^2 \rangle^{0.5}$) that shields the A−B blend interactions. Since $f_A$ = 0.75 DBCGPs are slightly farther from the interface, they have lower penetration into the blend domains than $f_A$ = 0.50 DBCGPs, decreasing their interfacial activity. Considering that $\gamma/\gamma_0$ of DBCGPs is comparable to $\gamma/\gamma_0$ of JGPs, with relatively easier synthesis of DBCGPs than JGPs, and that $\gamma/\gamma_0$ of DBCGPs is better than BCPs without the issues of micellization, DBCGPs are an attractive alternative to the industrial compatibilizer in immiscible homopolymer blends.

## SIMULATION

We model DBCGPs in an immiscible A and B homopolymer blend using a coarse-grained approach where the polymers are represented with the bead−spring model[19] with each bead representing a Kuhn segment within the polymer. The spherical particles are modeled by a shell of $d = 1\sigma$ ($\sigma \approx 1$ nm) noninteracting beads constrained as a rigid body. The monomers in the grafted AB diblock copolymers are chemically identical to the A and B monomers in the homopolymer blend. For the JGPs, A homopolymer chains are grafted on one hemisphere of the particle and an equal number of B homopolymer chains on the opposite hemisphere of the particle. Particle−particle, particle−polymer, and A−B interactions are modeled using the Weeks−Chandler−Andersen (WCA) potential.[20] The A−A and B−B nonbonded interactions are modeled using 6-12 Lennard-Jones (LJ) potential[21] with $\varepsilon = 1.0$ (in units of $k_BT$) and $\sigma = 1.0$ (in units of nm) shifted at $r_{cut} = 2.5\sigma$. The choice of these interactions leads to an immiscible blend with $\chi \sim 1$, and the two homopolymers macrophase separate within the simulation box.

To investigate DBCGP location in the blend we conduct Brownian dynamics (BD) simulations[22] in the isothermal isobaric (NPT) ensemble in a cubic simulation box with the $x$, $y$, and $z$ directions being coupled and varying by the same amount and same rate. To probe the interfacial properties of the blend with the compatibilizer, we run NPT-constant interfacial area simulations where the lengths of the simulation box in the $x$ and $y$ direction are held constant at $L_x = L_y = 60\sigma$ and a constant pressure of $P^* = 0.1$ is applied in the $z$ direction. Details of the model, simulation protocols, and analyses are described in the Supporting Information.



DOI: 10.1021/mz500793e
ACS Macro Lett. 2015, 4, 155−159

## ■ ASSOCIATED CONTENT

### Supporting Information

The details of the computational approach and additional results are presented. This material is available free of charge via the Internet at http://pubs.acs.org.

## ■ AUTHOR INFORMATION


### Corresponding Author

*E-mail: arthij@udel.edu.


### Notes

The authors declare no competing financial interest.

## ■ ACKNOWLEDGMENTS

We acknowledge financial support from the U.S. Department of Energy under Grant DE-SC0003912, the use of Janus supercomputer, supported by the NSF (award number CNS-0821794) and the CU Boulder, and use of NERSC supercomputing supported by the U.S. Department of Energy (DE-AC02- 05CH11231).

## ■ REFERENCES

(1) Utracki, L. A. *Commercial Polymer Blends*; Chapman and Hall: London, 1998; 83−136

(2) Shull, K. R.; Kramer, E. J.; Hadziioannou, G.; Tang, W. *Macromolecules* **1990**, *23* (22), 4780−4787.

(3) Noolandi, J.; Hong, K. M. *Macromolecules* **1982**, *15* (2), 482−492.

(4) Anastasiadis, S. H.; I, G.; Koberstein, J. T. *Macromolecules* **1989**, *22* (3), 1449−1453.

(5) Adedeji, A.; Lyu, S.; Macosko, C. W. *Macromolecules* **2001**, *34* (25), 8663−8668.

(6) Ginzburg, V. V. *Macromolecules* **2005**, *38* (6), 2362−2367.

(7) Foster, L. M.; Worthen, A. J.; Foster, E. L.; Dong, J. N.; Roach, C. M.; Metaxas, A. E.; Hardy, C. D.; Larsen, E. S.; Bollinger, J. A.; Truskett, T. M.; Bielawski, C. W.; Johnston, K. P. *Langmuir* **2014**, *30* (34), 10188−10196.

(8) Saigal, T.; Dong, H. C.; Matyjaszewski, K.; Tilton, R. D. *Langmuir* **2010**, *26* (19), 15200−15209.

(9) Walther, A.; Muller, A. H. E. *Chem. Rev.* **2013**, *113* (7), 5194−5261.

(10) Walther, A.; Matussek, K.; Muller, A. H. E. *ACS Nano* **2008**, *2* (6), 1167−1178.

(11) Wang, B. B.; Li, B.; Ferrier, R. C. M.; Li, C. Y. *Macromol. Rapid Commun.* **2010**, *31* (2), 169−175.

(12) Jiang, S.; Chen, Q.; Tripathy, M.; Luijten, E.; Schweizer, K. S.; Granick, S. *Adv. Mater.* **2010**, *22* (10), 1060−1071.

(13) Park, B. J.; Brugarolas, T.; Lee, D. *Soft Matter* **2011**, *7* (14), 6413−6417.

(14) Smoukov, S. K.; Gangwal, S.; Marquez, M.; Velev, O. D. *Soft Matter* **2009**, *5* (6), 1285−1292.

(15) Li, C. Z.; Benicewicz, B. C. *Macromolecules* **2005**, *38* (14), 5929−5936.

(16) Pyun, J.; Matyjaszewski, K.; Kowalewski, T.; Savin, D.; Patterson, G.; Kickelbick, G.; Huesing, N. *J. Am. Chem. Soc.* **2001**, *123* (38), 9445−9446.

(17) Koski, J.; Chao, H.; Riggleman, R. A. *Chem. Commun.* **2015**, DOI: 10.1039/C4CC08659G.

(18) Estridge, C. E.; J, A. *J. Polym. Sci., Part B: Polym. Phys.* **2015**, *53*, 76−88.

(19) Kremer, K.; Grest, G. S. *J. Chem. Phys.* **1990**, *92* (8), 5057−5086.

(20) Weeks, J. D.; Chandler, D.; Andersen, H. C. *J. Chem. Phys.* **1971**, *55* (11), 5422−+.

(21) Jones, J. E. *Proc. R. Soc. London A* **1924**, *106* (738), 463−477.

(22) Anderson, J. A.; Lorenz, C. D.; Travesset, A. *J. Comput. Phys.* **2008**, *227* (10), 5342−5359.



DOI: 10.1021/mz500793e
*ACS Macro Lett.* 2015, 4, 155−159